Mutational Analysis of Endonuclease V from *Thermotoga maritima*†

Jianmin Huang,‡,§ Jing Lu,‡,§,|| Francis Barany,‡ and Weiguo Cao*,‡,||

Department of Microbiology and Immunology, Hearst Microbiology Research Center and Strang Cancer Prevention Center, The Joan and Sanford I. Weill Medical College of Cornell University, 1300 York Avenue, Box 62, New York, New York 10021, and Department of Genetics and Biochemistry, South Carolina Experiment Station, Clemson University, 122 Long Hall, Clemson, South Carolina 29634-0324

Received November 19, 2001; Revised Manuscript Received April 28, 2002

ABSTRACT: Endonuclease V nicks damaged DNA at the second phosphodiester bond 3′ to inosine, uracil, mismatched bases, or abasic (AP) sites. Alanine scanning mutagenesis was performed in nine conserved positions of *Thermotoga maritima* endonuclease V to identify amino acid residues involved in recognition or endonucleolytic cleavage of these diverse substrates. Alanine substitution at D43, E89, and D110 either abolishes or substantially reduces inosine cleavage activity. These three mutants gain binding affinity for binding to double-stranded or single-stranded inosine substrates in the absence of a metal ion, suggesting that these residues may be involved in coordinating catalytic metal ion(s). Y80A, H116A, and, to a lesser extent, R88A demonstrate reduced affinities for double-stranded or single-stranded inosine substrates or nicked products. The lack of tight binding to a nicked inosine product accounts for the increased rate of turnover of inosine substrate since the product release is less rate-limiting. Y80A, R88A, and H116A fail to cleave AP site substrates. Their activities toward uracil substrates are in the following order: H116A > R88A > Y80A. These residues may play a role in substrate recognition. K139A maintains wild-type binding affinity for binding to double-stranded and single-stranded inosine substrate, but fails to cleave AP site and uracil substrate efficiently, suggesting that K139 may play a role in facilitating non-inosine substrate cleavage.

Endonuclease V is a DNA repair enzyme which hydrolyzes the second phosphodiester bond 3′ from inosine (*1*, *2*). In vivo, it is primarily involved in repair of inosine generated by adenine deamination (*3*). In vitro, endonuclease V is active toward AP site, uracil, and mismatches (*2*, *4*−*6*). With Mn^{2+} as the metal cofactor, the *Escherichia coli* endo V is also capable of cleaving insertions/deletions, and flap and pseudo-Y structures (*7*).

Endo V homologues have been found through genome sequencing in all three domains of life, eubacteria, archaea, and eukaryotes. Many thermophilic bacteria and archaea contain an endo V ortholog, suggesting its role in inosine repair due to accelerated adenine deamination at high temperatures. We have recently studied a cloned endo V homologue from the hyperthermophilic bacterium *Thermotoga maritima* and provided biochemical evidence that suggests its involvement in inosine repair (*1*). Our cleavage and binding analyses reveal that Tma[1] endo V retains extremely tight binding to nicked inosine product, essentially acting as a single-turnover inosine endonuclease. We propose that tight product binding may be required for the coordination of the downstream inosine repair process to prevent the generation of detrimental repair intermediates (*1*). Our binding studies suggest that endo V may fail to compete with other uracil DNA glycosylases for a uracil base and, therefore, plays no significant physiological role in uracil repair (*1*, *3*).

Tma endo V efficiently binds to and cleaves single-stranded inosine substrate as well (*1*). It appears that Tma endo V is well-adapted for interacting with single-stranded inosine-containing sequences, thereby allowing the accommodation of two enzyme molecules to bind to an inosine-inosine base pair. As a result, when enzyme is in excess of substrate, endo V may cleave the complementary strand opposite of inosine, AP site, and uracil substrates, resulting in a double-strand break. This notion is in keeping with previous genetic analysis (*3*). Our biochemical analyses suggest that endo V may sense both local helical abnormality and base difference during the recognition process, which may account for the cleavage specificity toward different DNA species (*1*).

Endonuclease V cleaves A- and G-containing strands in a mismatch more efficiently than T- or C-containing mismatches (*1*). A scheme for detection of known mutations

† This work was supported by grants from the National Institutes of Health (PO1-CA65930-02-04 and R01-CA81467-01), the Ralph E. Powe Junior Faculty Enhancement Award from Oak Ridge Associated Universities, and the South Carolina Experiment Station.

* To whom correspondence should be addressed. E-mail: wgc@clemson.edu. Telephone: (864) 656-4176. Fax: (864) 656-6879.

‡ The Joan and Sanford I. Weill Medical College of Cornell University.

§ These authors contributed equally to this work.

|| Clemson University.

[1] Abbreviations: BSA, bovine serum albumin; dNTP, deoxyribonucleoside triphosphate; DTT, dithiothreitol; 6-Fam, 6-carboxyfluorescein; HEPES, *N*-(2-hydroxyethyl)piperazine-*N*′-2-ethanesulfonic acid; PAGE, polyacrylamide gel electrophoresis; PCR, polymerase chain reaction; SDS, sodium dodecyl sulfate; PMSF, phenylmethanesulfonyl fluoride; Tet, 4,7,2′,7′-tetrachloro-6-carboxyfluorescein; Tma, *T. maritima*; wt, wild-type.

10.1021/bi015960s CCC: $22.00
Published on Web 06/04/2002

Chart 1

```
5'-Fam-TA CCC CAG CGT CTG CGG TGT TGC GTI AGT TGT CAT AGT TTG ATC CTC TAG TCT TGT TGC GGG TTC C-3'
      3'- GGG GTC GCA GAC GCC ACA ACG CAA TCA ACA GTA TCA AAC TAG GAG ATC AGA ACA ACG CCC-Tet-5'
```

termed the mutation identification DNA analysis system relies on a T/G DNA glycosylase and endonuclease V to cleave a synthetic probe in a PCR-less fashion (*8*). More recently, we have developed a mutation scanning assay using Tma endo V in combination with a thermostable ligase for detection of unknown point mutations and insertion/deletion mutations in BRCA1, BRCA2, p53, K-*ras*, VHL, and APC genes (*9*). This mutation scanning assay is sufficiently sensitive to detect K-*ras* mutations diluted 1:20 with wild-type DNA, a p53 mutation on a 1.7 kb amplicon, and unknown p53 mutations in pooled DNA samples (*9*).

Despite extensive biochemical investigation of *E. coli* and Tma endonuclease V, the structural basis underlying its diverse substrate recognition and cleavage properties is still unknown. In this study, an alanine scanning analysis was performed at nine conserved amino acid residues on Tma endo V. D43, D110, and possibly E89 were identified as the putative active site residues responsible for coordinating metal ion(s). Y80, R88, and H116 play a role in substrate recognition. K139A affects cleavage of non-inosine substrates such as AP site and uracil.

EXPERIMENTAL PROCEDURES

Reagents, Media, and Strains. All routine chemical reagents were purchased from Sigma Chemicals (St. Louis, MO) or Fisher Scientific (Fair Lawn, NJ). Restriction enzymes and T4 DNA ligase were purchased from New England Biolabs (Beverly, MA). DNA sequencing kits and PCR kits were purchased from the Applied Biosystems Division of Perkin-Elmer Corp. (Foster City, CA). BSA, dNTPs, and ATP were purchased from Boehringer-Mannheim (Indianapolis, IN). *Pfu* DNA polymerase was purchased from Stratagene (La Jolla, CA). Deoxyoligonucleotides were ordered from Integrated DNA Technologies Inc. (Coralville, IA). MOPS medium was prepared as described previously (*10*). Tma endo V sonication buffer consisted of 20 mM HEPES (pH 7.4), 1 mM EDTA (pH 8.0), 0.1 mM DTT, 0.15 mM PMSF, and 50 mM NaCl. *Taq*I storage buffer (1×) consisted of 50% glycerol, 10 mM Tris-HCl (pH 8.0), 1 mM EDTA (pH 8.0), 1 mM DTT, and 0.2 mg/mL BSA. GeneScan stop solution consisted of 80% formamide (Amresco), 50 mM EDTA (pH 8.0), and 1% blue dextran (Sigma Chemicals). TB buffer (1×) consisted of 89 mM Tris and 89 mM boric acid. TE buffer consisted of 10 mM Tris-HCl (pH 8.0) and 1 mM EDTA. *E. coli* host strain AK53 (*mrr*B$^-$, MM294) was from our laboratory collection.

Alanine Scanning Mutagenesis. An overlapping extension PCR procedure was used for site-directed mutagenesis (*11*). PCR products digested with a pair of *Nde*I and *Spe*I endonucleases were ligated to cloning vector pEV5 treated with the same pair of restriction endonucleases. The ligated vectors were transformed into *E. coli* strain AK53 (*mrr*B$^-$, MM294). Plasmids containing inserts were reisolated and sequenced on an ABI sequencer using Dye-dideoxy terminator chemistry to identify mutated sequence and ensure that the constructs were free of PCR error. Strains containing mutated Tma endonulcease V (*nfi*) genes were expressed in 5 mL of MOPS medium supplemented with 50 μg/mL ampicillin (*10*) at 37 °C overnight. Cell pastes were suspended in 300 μL of sonication buffer and sonicated for 4 × 10 s at 4 °C using a Sonifier Cell Disruptor 350 (Branson). After cell debris had been removed by centrifugation, the supernatants containing Tma endonuclease V proteins were incubated at 70 °C for 15 min to inactivate host proteins. The denatured proteins were separated from soluble Tma endonuclease V proteins by centrifugation. The protein concentrations of Tma endonuclease V mutants were quantified by scanning a 12.5% SDS−PAGE gel loaded with known amounts of wild-type Tma endonuclease V. Further purification was conducted by ion exchange chromatography using a 5 mL HiTrap SP column as described previously (*1*). Purified proteins were diluted to 1 μM with 1× *Taq*I storage buffer and stored at −20 °C prior to use.

DNA Cleavage Reaction. The fluorescence labeled deoxyoligonucleotide substrates were prepared as described (*1*). The sequence of a typical inosine substrate is shown in Chart 1. A nicking event at the top strand generates a 27 nt (nucleotide) labeled product, while that at the bottom strand generates a 38 nt labeled product. The cleavage reactions were performed at 65 °C for 30 min in a 20 μL reaction mixture containing 10 mM HEPES (pH 7.4), 1 mM DTT, 2% glycerol, 5 mM $MgCl_2$ unless otherwise specified, 10 nM DNA substrate, and the indicated amount of purified Tma endonuclease V protein. The reaction was terminated by adding an equal volume of GeneScan stop solution. The reaction mixtures were then heated at 94 °C for 2 min and cooled on ice. Samples (3 μL) were loaded onto a 10% GeneScan denaturing polyacrylamide gel (Perkin-Elmer). Electrophoresis was conducted at 1500 V for 1 h using an ABI 377 sequencer (Perkin-Elmer). Cleavage products and remaining substrates were quantified using GeneScan analysis software version 2.1 or 3.0.

Gel Mobility Shift Assay. The binding reaction mixture contains 100 nM double-stranded fluorescence-labeled oligonucleotide DNA substrates, 5 mM $MgCl_2$ or $CaCl_2$ or 2 mM EDTA, 20% glycerol, 10 mM HEPES (pH 7.4), 1 mM DTT, and 75 nM Tma endonuclease V protein. The binding reactions were carried out at 65 °C for 30 min. Samples was electrophoresed on a 6% native polyacrylamide gel in 1× TB buffer supplemented with 10 mM $MgCl_2$ or $CaCl_2$ or 2 mM EDTA. The bound and free DNA species were analyzed using FluorImager 595 (Molecular Dynamics) with the following settings: PMT at 1000 V, excitation at 488 nm, and emission at 530 nm (530 DF30 filter). Data analysis was carried out using ImageQuaNT version 4.1 (Molecular Dynamics).

RESULTS

DNA Cleavage. To identify amino acid residues which may play an important functional role in endonuclease V, we aligned four representative endo V homologues from bacteria, archaea, and eukaryotes (Figure 1). We selected nine conserved residues that we considered to be candidates for roles in metal binding, catalysis, and substrate recognition

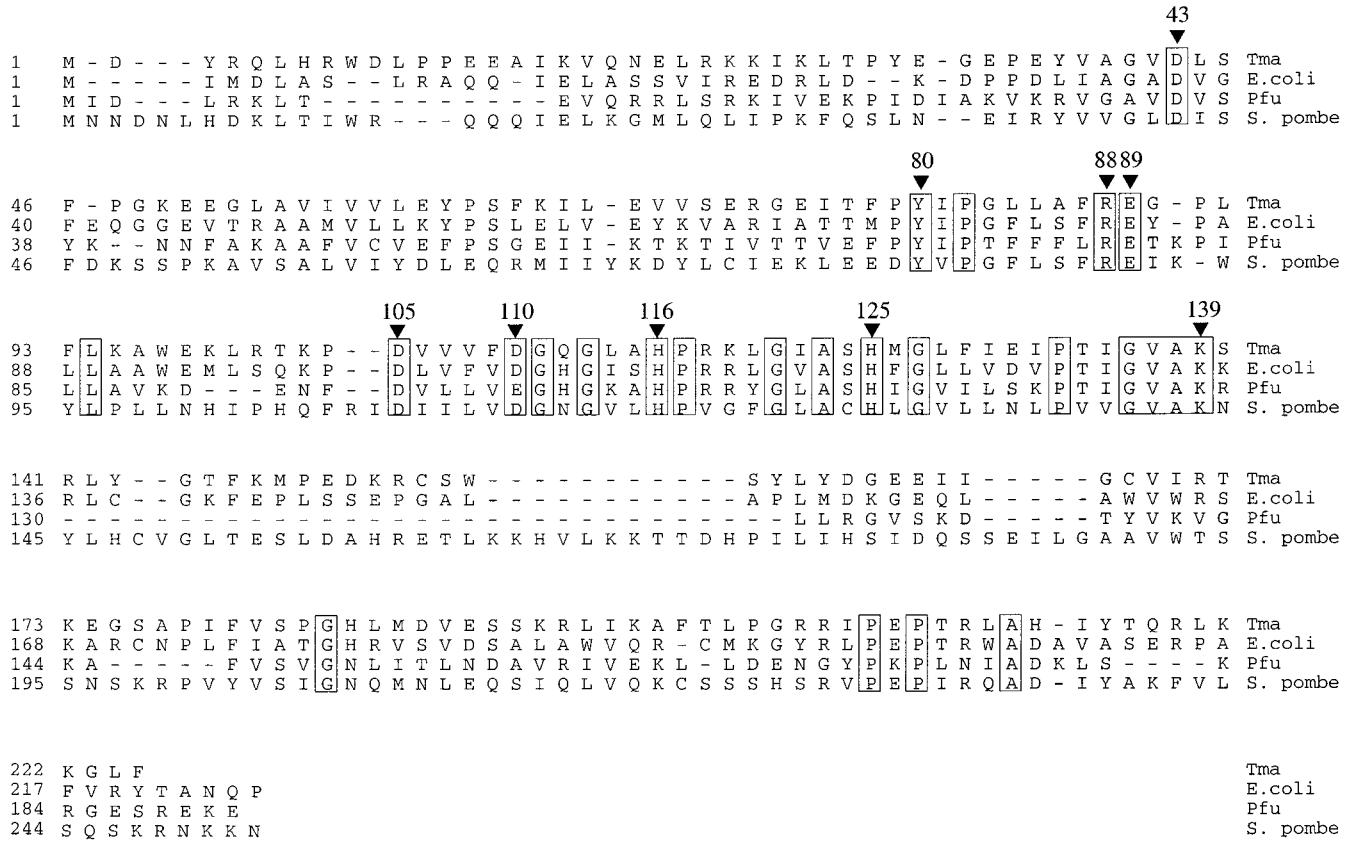

FIGURE 1: Alignment of representative endonuclease V orthologs from eubacteria, archaea, and eukaryotes: E. coli, *Escherichia coli*; Tma, *Thermotoga maritima*; Pfu, *Pyrococcus furiosus*; S. pombe, *Schizosaccharomyces pombe*. (▼) Sites chosen for alanine scanning mutagenesis.

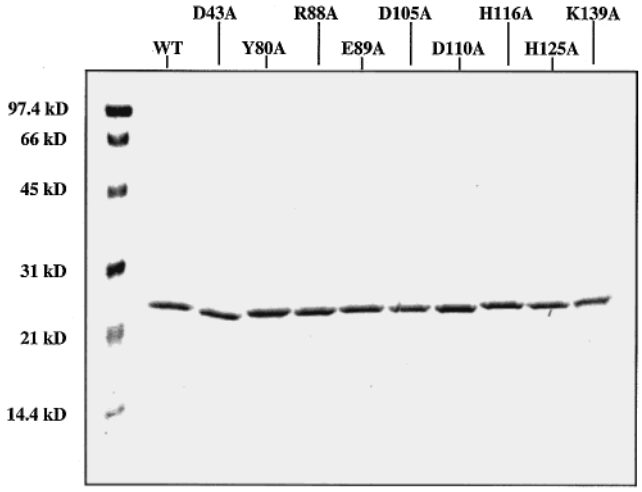

FIGURE 2: SDS−PAGE analysis of the wt and mutant proteins. Purified proteins (~3 μg) were electrophoresed on a 15% polyacrylamide gel containing 0.1% SDS. Protein bands were visualized by Coomassie staining (*24*).

for alanine scanning mutagenesis. For example, the acidic residues were chosen for their potential role in metal ion coordination. Tma endo V mutants were generated through an overlapping PCR procedure and partially purified through heat treatment at 75 °C for 15 min. The resulting mutant proteins are devoid of the indigenous *E. coli* endonuclease V (*1*). The wt and mutant proteins were purified by ion exchange chromatography (Figure 2). The cleavage assays were performed using oligonucleotide substrates fluorescently labeled at both strands (Figure 3A). Our previous studies have shown that wild-type Tma endo V nicks at inosine sites. When the enzyme is in excess, it cleaves the complementary strand opposite the inosine-containing strand (*1*). To ensure various cleavage activities are revealed (inosine strand, complementary strand, and nonspecific sites), the wt and mutant enzymes were subjected to cleavage reactions with enzyme in excess (10:1). As expected for wild-type Tma endonuclease V, we observed a blue band which represented the top inosine cleavage product and a green band which represented the bottom complementary strand cleavage product (Figure 3B). Some lower-molecular mass nonspecific cleavage products were also observed. Even with 10-fold enzyme excess over substrate, D43A and D110A did not show any DNA endonuclease activity for cleaving either of the strands. E89A exhibited 20% cleavage of the inosine strand with no detectable cleavage of the complementary strand (Figure 3B,C). Y80A, R88A, H116A, and K139A maintained efficient cleavage toward the inosine strand but lost complementary strand cleavage activity. The cleavage patterns generated by D105A and H125A were essentially identical to that of the wt enzyme, exhibiting cleavage toward both the inosine-containing strand and the complementary strand in the double-stranded substrate (Figure 3B,C). To more precisely compare the difference in inosine cleavage activity, the specific activity was measured under the conditions in which the substrate was in excess. Most of the mutants except for D43A, E89A, and D110A exhibited a similar level of specificity for the wt enzyme [0.32 fmol of product min^{-1} (fmol of enzyme)$^{-1}$]. D43A, E89A, and D110A did not show detectable inosine endonuclease activity under conditions in which the substrate was in excess, suggesting that they are essential for endonuclease

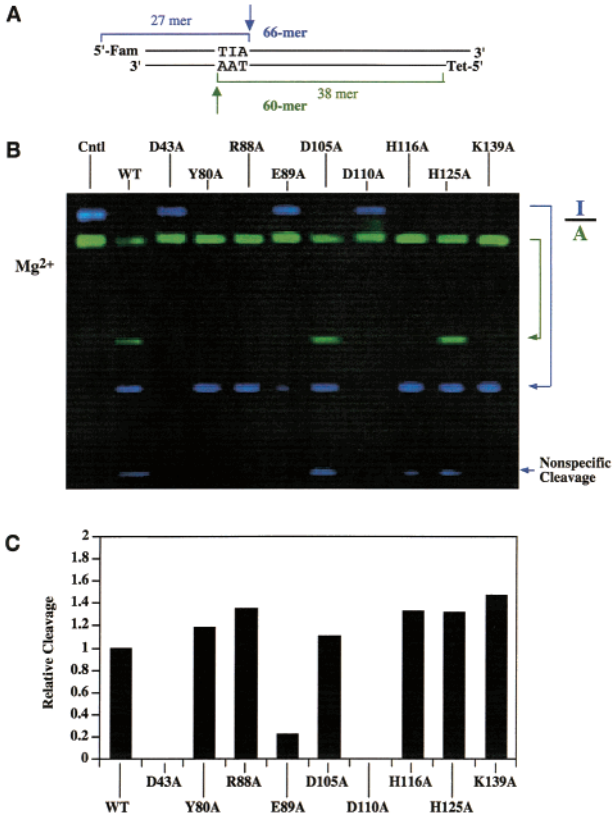

FIGURE 3: Cleavage activities of Tma endonuclease V mutants on a double-stranded inosine-containing substrate (I/A). (A) Substrate and cleavage sites. The inosine-containing strand (top strand) is Fam-labeled, and the opposite strand (bottom strand) is Tet-labeled. Cntl represents a substrate control. (B) The cleavage reactions were performed as described in Experimental Procedures with an E:S (enzyme:substrate) ratio of 10:1 ([S] = 10 nM) in the presence of 5 mM $MgCl_2$. (C) Relative cleavage of the inosine strand. The intensity of the cleavage product from the inosine strand (blue) was quantified. The intensity of the cleavage product from the wt enzyme was taken to be 1.0.

V function. Mn^{2+} enhanced nonspecific cleavage activity, but the overall cleavage profiles of the mutants remained similar to that of Mg^{2+} (not shown).

Binding to Inosine Substrate. We used a previously developed fluorescence-based gel mobility shift assay to compare substrate binding among the nine alanine-substituted mutants (*1*). As previously reported, wt Tma endo V formed a detectable but diffuse shifted complex with the inosine substrate in the absence of a metal cofactor (ref *1* and Figure 4A). Interestingly, the two catalytically inactive mutants, D43A and D110A, now formed a distinct complex with the inosine substrate. Although not observed in most mutational studies performed on endonucleases, the restriction endonuclease *Mun*I does show such a peculiar property; i.e., elimination of the negative charges at some metal binding residues confers binding specificity to the cognate sequence (*12*). It is suggested that the negative charges may cause electrostatic repulsion between the carboxylates and the phosphate in the absence of a neutralizing metal ion. By substituting the negatively charged Asp or Glu with Ala, the mutants become capable of binding to the cognate sequence even without a metal ion. A similar notion can be applied to explain the binding behavior of D43A and D110A mutants, which implies that D43A and D110A are involved in the coordination of a divalent metal ion required for catalysis.

In the presence of a metal cofactor such as Mg^{2+} or Ca^{2+}, most of the mutants exhibited an affinity for binding to the double-stranded inosine substrate comparable to that of the wt enzyme (Figure 4B). Since Ca^{2+} only supports binding but not catalysis (*1*), the shifted bands represent an ES (enzyme−substrate) complex. The shifted bands observed with Mg^{2+}, on the other hand, may represent an enzyme-nicked product complex due to strand cleavage. Apparently, Y80A, R88A, E89A, and H116A no longer bind to the intact inosine substrate as tightly as the wt enzyme as judged by gel shift data with Ca^{2+} (Figure 4B). Further, the gel shift data with Mg^{2+} suggested that Y80A, E89A, and H116 may have reduced affinity for binding to the nicked product as well (Figure 4C). To more definitively assess the impact of alanine-substituted mutants had on endonuclease binding to the nicked product, we performed gel mobility shift analysis using a synthesized inosine oligonucleotide substrate with a preexisting nick (Figure 5). It is evident from the gel shift experiments with Ca^{2+} that Y80A, R88A, E89A, and H116A failed to bind to the nicked inosine product as tightly as the wt enzyme (Figure 5A). In the presence of the catalytically competent metal ion Mg^{2+}, a reduced level of binding was observed with E89A (Figure 5B). Y80A did not remain bound to the nicked product with a sufficiently long half-life to allow the detection of a distinct band shift (Figure 5A,B). These results suggested that some endo V variants such as Y80A, E89A, and H116A may have affected both ES and EP binding, while R88A may primarily have affected product release.

A time course analysis was performed to assess how the altered binding behavior changed the cleavage kinetics of the inosine-containing strand in a double-stranded sequence. When the enzyme is in deficit (1:10 E:S ratio), the wt enzyme only cleaved a limited amount of the substrate as it remained bound to the nicked product (Figure 6). Likewise, the mutant H125A, which showed wt level cleavage activity and binding, also failed to turn over this inosine-containing double-stranded substrate. The three mutants Y80A, R88A, and H116A, which showed reduced affinities for the nicked inosine substrate by gel mobility shift analysis (Figure 5), now were able to release the product and nicked the inosine strand in a multiple-turnover fashion (Figure 6A). The plateau effect observed with R88A and H116A is likely due to the loss of enzymatic activity during extended incubation (not shown). Most prominently, the cleavage reaction by Y80A proceeded close to completion with an apparent first-order rate constant of 0.04 min^{-1}. The kinetic analysis, combined with the binding data, suggests that some of the mutants (as represented by Y80A) have changed the reaction kinetics by increasing the product release rate constant k_3 to facilitate multiple turnover (Figure 6B).

For wt Tma endonuclease V, one would expect to see an initial burst phase because of the limited product release (*13*, *14*). To prove that Tma endo V follows the burst kinetics, the cleavage reactions were monitored under conditions in which the E:S ratios were 1:10 and 2:10. Kinetic analysis indicates that Tma endo V indeed follows the burst kinetics (Figure 7). The amount of nicked product increased 2-fold when the enzyme concentration was doubled (Figure 7). Burst kinetics behavior allows the active site concentration to be titrated (*13*, *14*). It appeared that 100% of the thermostable endo V molecules were active.

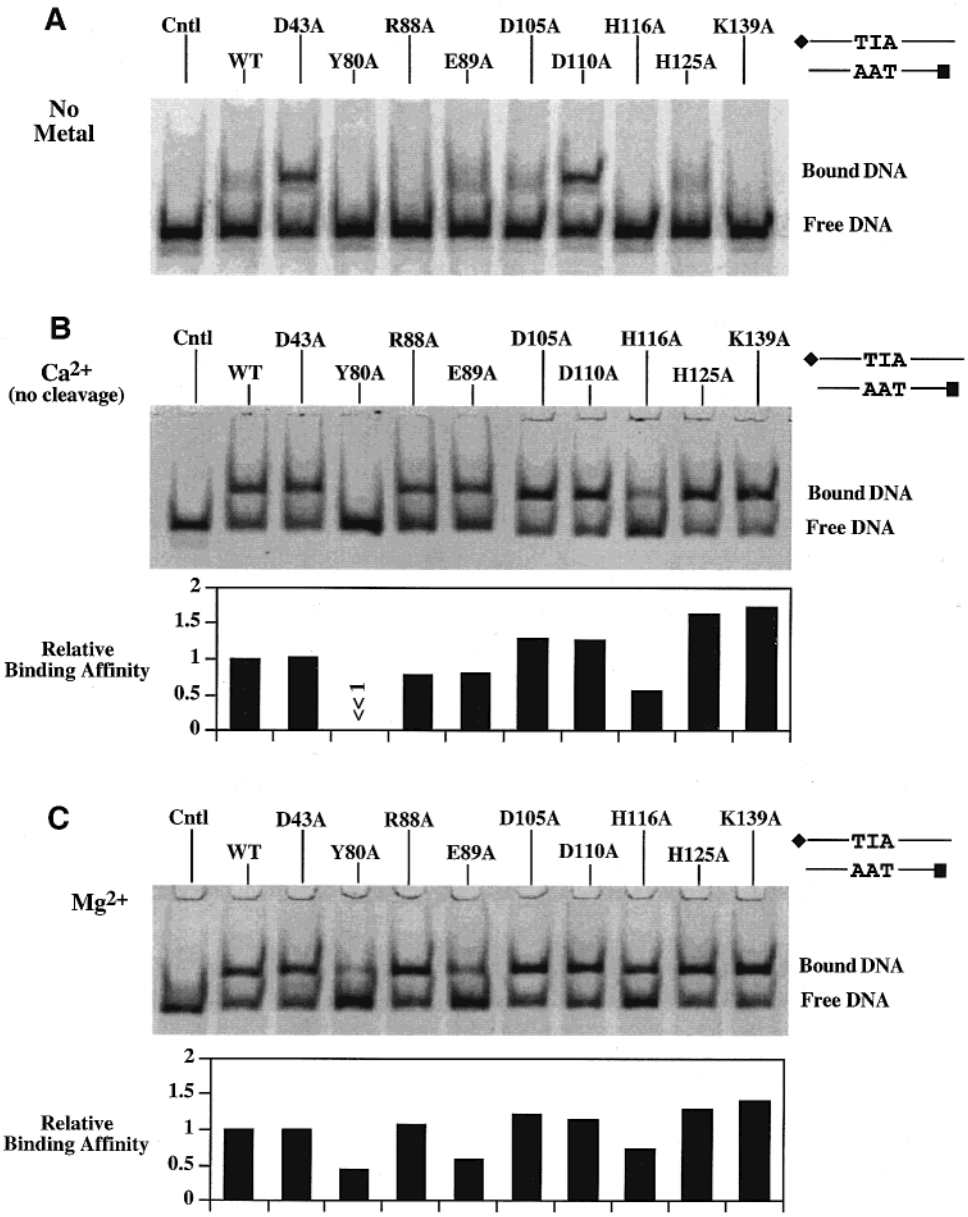

FIGURE 4: Gel mobility shift of Tma endonuclease V mutants with inosine-containing substrates. Cntl represents a substrate control. (A) Gel mobility shift assays were performed with an inosine-containing double-stranded substrate (I/A) as described in Experimental Procedures except that $MgCl_2$ was replaced with 2 mM EDTA. (B) Gel mobility shift assays with an inosine-containing double-stranded substrate (I/A) in the presence of $CaCl_2$. (C) Gel mobility shift assays with an inosine-containing double-stranded substrate (I/A) in the presence of $MgCl_2$. The bound DNA ([ES]) and remaining free DNA ([S]) were quantified using Quantity One (Bio-Rad). The apparent K_d values were calculated with the relation $K_d = ([E]_T - [ES])([S]/[ES])$, where $[E]_T$ is the total enzyme concentration. The K_d-wt/K_d-mutant ratio was taken to be the relative binding affinity. A higher ratio indicates tighter binding.

Cleavage and Binding of Single-Stranded Inosine Substrate. To assess the single-stranded endonuclease activity, we examined cleavage using fluorescently labeled (Tet) inosine-containing single-stranded oligonucleotide. Most of the endo V variants retained wt cleavage activity toward the single-stranded inosine-containing substrate (Figure 8A). Consistent with the cleavage results obtained using the double-stranded inosine-containing substrate (Figure 3), E89A had only ~2% cleavage activity while D43A and D110A were inactive toward the single-stranded inosine-containing substrate (Figure 8A). The binding of the single-stranded inosine-containing substrate also required a metal cofactor for most of the mutants. D43A, D110A, and E89A, however, were able to bind to the single-stranded inosine-containing substrate without a metal ion (Figure 8B), suggesting a similar interaction among the enzyme, inosine substrate, and metal ion for both single-stranded and double-stranded substrates. The formation of a distinct shifted band by E89A in the absence of a metal ion using the single-stranded inosine substrate suggests that E89 may play an analogous role in metal binding similar to the roles of D43 and D110 (Figures 4A and 8B).

The binding pattern of the single-stranded inosine-containing substrate in the presence of Ca^{2+} is essentially identical to that of the double-stranded substrate; i.e., most of the mutants bound to the substrate at least as strong as the wt enzyme. Y80A and H116A again exhibited a reduced level of binding to the inosine substrate (Figure 8C). In the presence of Mg^{2+}, Y80A exhibited an intense lower-molecular mass band with concurrent disappearance of the

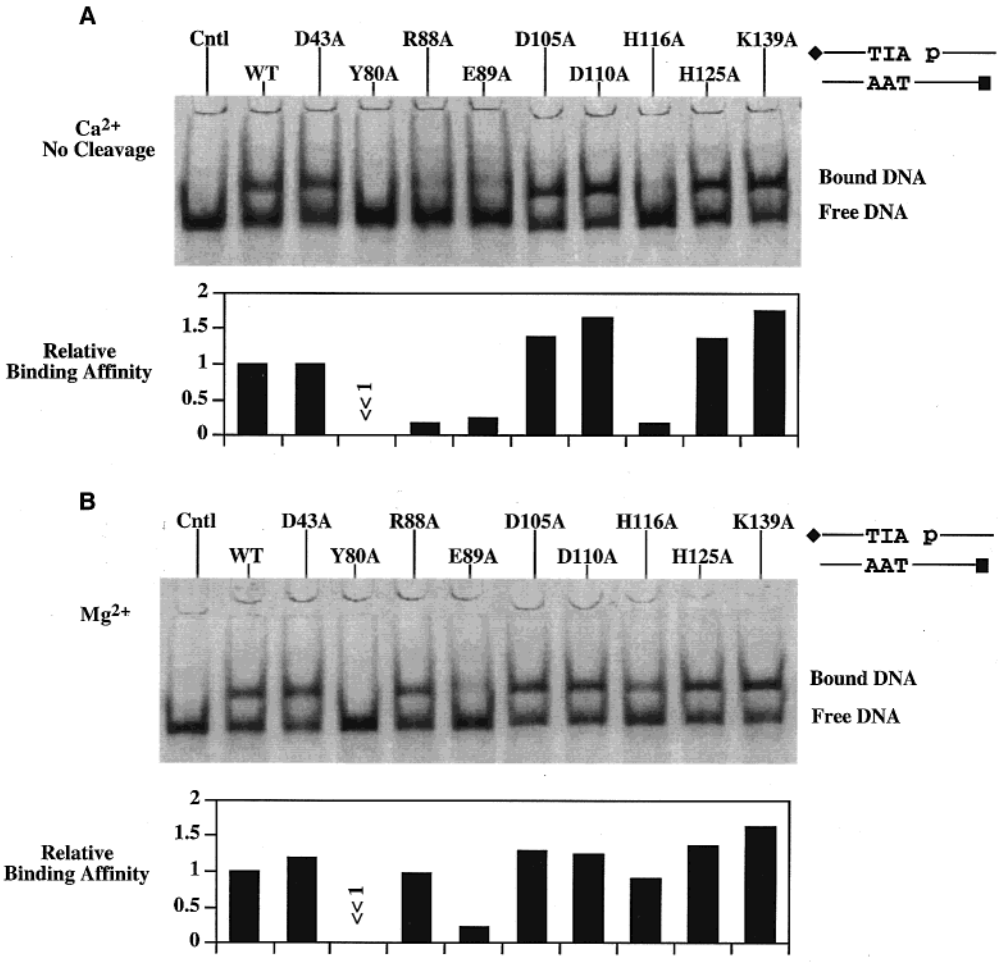

FIGURE 5: Gel mobility shift of Tma endonuclease V mutants with the nicked inosine product. Cntl represents a substrate control. (A) Gel mobility shift assays with a nicked inosine-containing double-stranded product (I/A) in the presence of $CaCl_2$. (B) Gel mobility shift assays with a nicked inosine-containing double-stranded product (I/A) in the presence of $MgCl_2$. The relative binding affinity was calculated as described in the legend of Figure 4.

free DNA band, suggesting that most of the single-stranded substrate was cleaved and released (Figure 8D). Given the reduced level of binding seen with Ca^{2+}, it is likely that Y80A no longer binds to the single-stranded nicked product tightly, thereby dissociating from the product. Some of the mutants, such as D105A and K139A, may prevent release of the single-stranded nicked product because of tighter binding (Figure 8D). D43A, D110A, and E89A exhibited little cleavage activity toward the inosine substrate (Figure 8A). As expected, they formed a distinct stable complex as seen by the mobility shift gel (Figure 8D). However, they migrated faster than the wt and other catalytically active endo V mutants. One scenario for explaining the different migration patterns is one in which the binding of the wt enzyme and some other active mutants may cause bending of the nicked inosine product (Figure 8D), resulting in a slower migration (*15*). D43A, D110A, and E89A mutants may have lost the ability to bend the DNA due to the loss of the negative charges, resulting in a faster migration.

Cleavage of Uracil and AP Site Substrates. We assessed uracil endonuclease activity of Tma endo V mutants using A/U, G/U, and T/U substrates. D43A, D110A, and E89A were inactive toward any of the uracil substrates, which is consistent with the proposed metal binding role (Figure 9A–C). D105A, which was active toward various inosine substrates, was also active toward uracil-containing substrates. H125A cleaved G/U and T/U substrates efficiently (Figure 9B,C); however, its cleavage activity against the perfectly base-paired substrate A/U was halved compared to that of the wt enzyme (Figure 9A). Y80A was inert toward A/U and G/U substrates and showed minimal cleavage toward T/U. R88A, H116A, and K139A exhibited a reduced level of uracil cleavage. The degree of uracil cleavage by these three mutants appeared to be affected by the nature of the base pair. When the substrate contained a Watson–Crick base pair such as A/U (Figure 9A), the uracil cleavage activity was lowest. When the substrate contained a mismatch such as G/U or T/U, the uracil cleavage activity was enhanced (Figure 9B,C). These results are in keeping with our previous time course analysis of the wt enzyme using A/U and T/U substrates (*1*), suggesting that a uracil in a locally distorted mismatch environment provides a better signal for base recognition.

We assessed 3′ AP endonuclease activity of Tma endo V mutants using the A/AP substrate. *E. coli* endonuclease IV is a thermostable 5′ AP endonuclease (*16*). To prevent the interference of the host AP endonuclease, we further purified the wt and mutant endo V by HiTrap SP column chromatography (Amersham Pharmacia Biotech). Significant 3′ AP endonuclease activity was observed only with D105A and H125A (Figure 9D), both of which had consistently exhibited wt DNA cleavage activities toward other substrates.

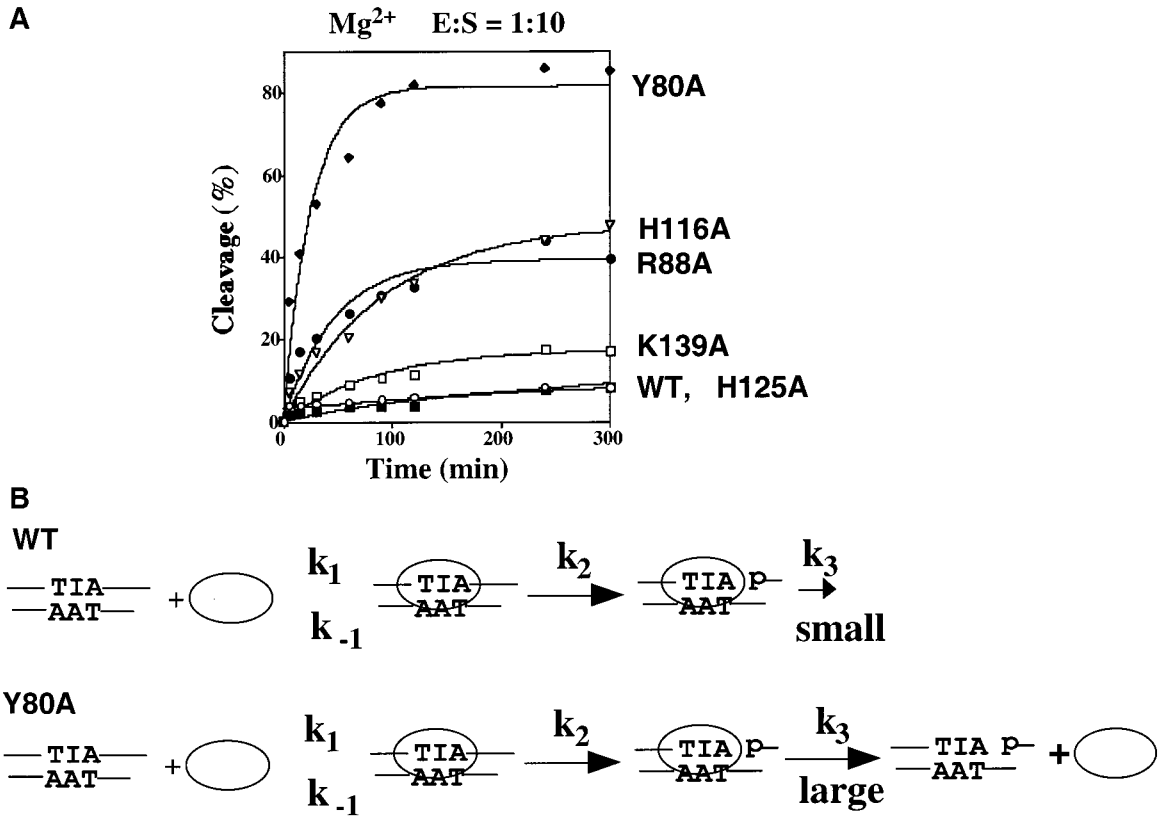

FIGURE 6: Time-course analysis of inosine cleavage by Tma endo V mutants. The cleavage reactions were performed as described in Experimental Procedures with an E:S (enzyme:substrate) ratio of 1:10 ([S] = 10 nM) in the presence of 5 mM $MgCl_2$. Reactions were terminated at specific time points for GeneScan analysis. The ovals represent Tma endo V.

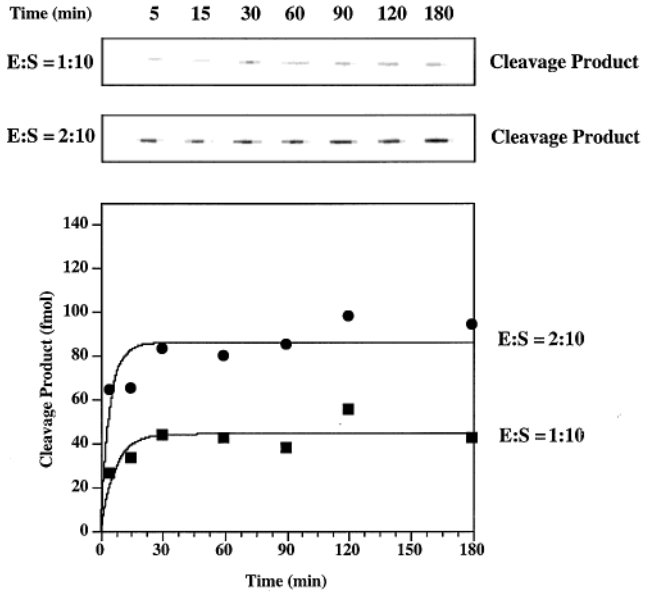

FIGURE 7: Active site titration of wt Tma endonuclease V. The inosine strand cleavage reactions were performed as described in Experimental Procedures with E:S (enzyme:substrate) ratios of 1:10 and 2:10 ([S] = 10 nM) in the presence of 5 mM $MgCl_2$. Reactions were terminated at specific time points for GeneScan analysis.

Some minimal AP endonuclease activity was observed with H116A, but all other mutants abrogated AP cleavage (Figure 9D).

DISCUSSION

This work examines the role played by conserved residues in the diverse activities exhibited by endonuclease V. Alanine mutations introduced at seven positions dramatically affect endonuclease V activities. To understand the effects of these mutations, we analyzed DNA cleavage activities using inosine, uracil, and AP site oligonucleotide substrates, and assessed binding affinity by gel mobility assays using double-stranded and single-stranded inosine substrates. This study provides insights into the active site organization and DNA recognition of endonuclease V.

Metal Binding and the Active Site (D43, D110, and E89). It is known from biochemical studies that endonuclease V is a metal-dependent DNA endonuclease (*1*, *2*). The enzyme is most active with Mg^{2+} or Mn^{2+} as the metal cofactor. Our previous binding studies have demonstrated that a divalent metal ion is required not only for catalysis but also for formation of a stable enzyme−substrate complex (*1*). For many endonucleases, a few negatively charged amino acid residues such as Asp and Glu are involved in metal binding (*17*−*19*). Of four such residues we chose to study, three of them (D43, D110, and E89) appear to be important for coordinating metal ion(s). D43A and D110A abolish the endonuclease activities toward all substrates we have tested, which include double-stranded and single-stranded inosine substrates (Figure 3) and double-stranded uracil and AP site substrates (Figure 9). E89A had only ~20% catalytic activity toward double-stranded inosine substrates (Figure 3C). Most interestingly, D43A and D110A, and in some case E89A, bind to inosine substrates in the absence of a metal ion (Figures 4A and 8B). D83A and E98A in restriction endonuclease *Mun*I have shown a similar binding behavior (*12*). More recently, the *Mun*I crystal structure complexed with cognate DNA positions D83A and E98A at the active

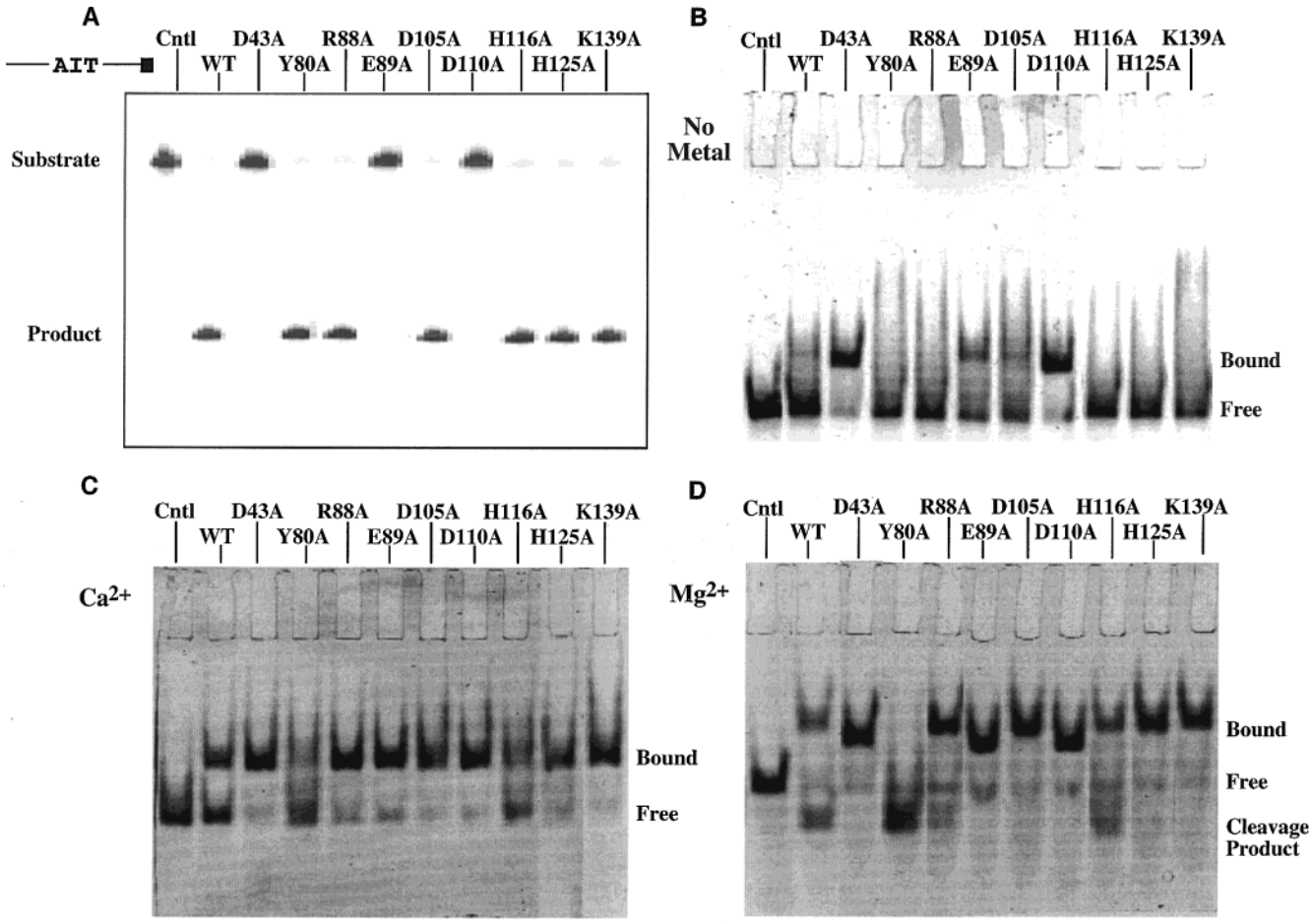

FIGURE 8: Binding and cleavage of the single-stranded inosine substrate. Cntl represents a substrate control. (A) Cleavage by Tma endo V mutants. The cleavage reactions were performed as described in Experimental Procedures with an E:S (enzyme:substrate) ratio of 1:1 ([S] = 10 nM) in the presence of 5 mM $MgCl_2$. (B) Gel mobility shift of Tma endo V mutants without a metal cofactor. (C) Gel mobility shift of Tma endo V mutants with 5 mM $CaCl_2$. (D) Gel mobility shift of Tma endo V mutants with 5 mM $MgCl_2$.

site (*20*). It is likely that D43 and D110 in Tma endo V, and possibly E89, are involved in binding catalytic metal(s) for the hydrolysis of the scissile phosphate bond. Ca^{2+} competition has been used as a probe to assess the numbers of metal ions involved in DNA cleavage by *Eco*RV (*21*, *22*). A stimulatory effect by Ca^{2+} on cognate site cleavage has been taken as an indication of a two-metal catalytic mechanism. We have not observed any enhancement of inosine cleavage in $Ca^{2+}-Mg^{2+}$ competition (not shown). Thus, the number of metal ions involved in strand cleavage in endonuclease V remains to be determined.

Y80. Alanine substitution at Y80 substantially reduced the affinity of endo V for the double- and single-stranded inosine substrate (Figures 4 and 8), as well as the nicked inosine product (Figure 5). Evidently, weak binding helps endo V dissociate from the product, thereby allowing rapid turnover of the inosine substrate (Figure 6). The loss of AP endonuclease and uracil endonuclease activities may also be attributed to a weaker binding affinity (Figure 9). These results suggest that Y80 plays an important role in maintaining a stable complex between the enzyme and the repair intermediate. Y80 may play such a role by making direct contact with the substrate and the product through base contact or phosphate−backbone interaction, or by organizing a network of contacts mediated by other amino acid residues. The kinetic property of accelerated product release is analogous to that of R177A in human AP endonuclease APE1 (*23*). In a DNA-bound structure, R177 makes a direct contact with the 3′ phosphate at the AP site to lock APE1 onto the AP site (*23*). Thus, a phosphate−backbone contact may contribute to tight product binding.

R88 and H116. R88A and H116A exhibit similar properties. Both of these variants show reduced affinity for the double-stranded inosine substrate and nicked product (Figures 4 and 5), which results in an enhanced turnover (Figure 6). They maintain wt level single-stranded inosine cleavage activity (Figure 8). The major difference between R88A and H116A is at uracil substrates. H116A is ~4-fold more active than R88A for the G/U substrate and 2.5-fold more active for the T/U substrate (Figure 9). Apparently, R88 plays a more important role in uracil recognition.

K139. Alanine substitution at K139 has little effect on binding (Figures 4 and 5). K139A maintains wt level cleavage activity toward the double-stranded inosine substrate I/A (Figure 3). Like the wt enzyme, K139A remains bound even after cleaving inosine substrate due to tight product binding (Figure 6). The main effect of K139A substitution on endo V is at cleavage of non-inosine substrates. In addition to the lack of AP endonuclease activity, K139A has a substantially reduced uracil endonuclease activity (Figure 9). A more detailed kinetic analysis is required to understand the precise catalytic role K139 may play in substrate recognition and/or catalysis.

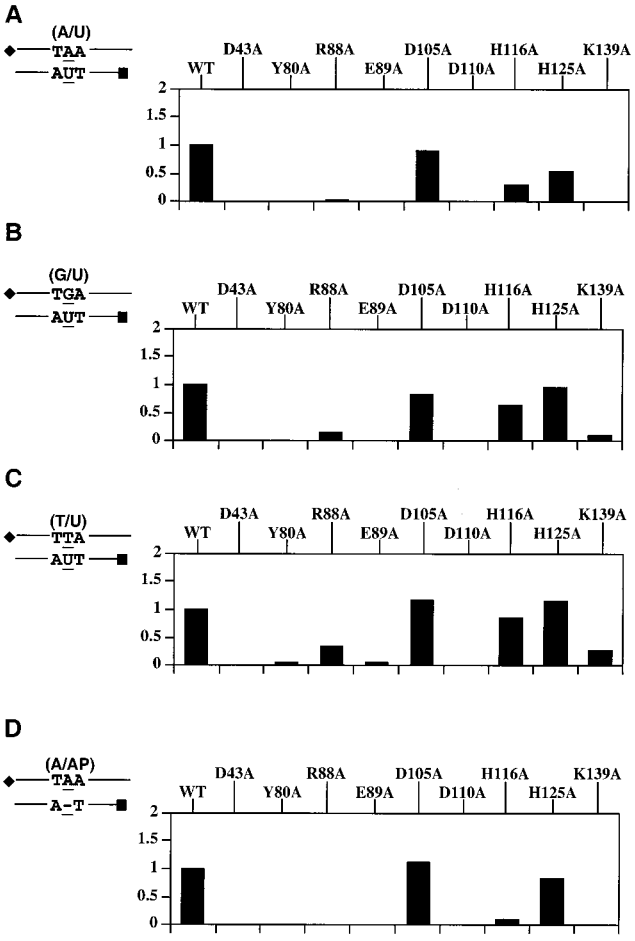

FIGURE 9: Cleavage activities of Tma endo V mutants on uracil and AP site substrates. The cleavage reactions were performed as described in Experimental Procedures with an E:S (enzyme: substrate) ratio of 10:1 ([S] = 10 nM) in the presence of 5 mM $MgCl_2$. Cntl represents a substrate control. (A) Cleavage of the uracil-containing strand with A/U substrate. (B) Cleavage of the uracil-containing strand with G/U substrate. (C) Cleavage of the uracil-containing strand with T/U substrate. (D) Cleavage of the AP-containing strand with AP site substrate (A/AP). The cleavage products were quantified using Quantity One (Bio-Rad). The intensity of the cleavage product generated by the wt enzyme was taken to be 1.0.

To elucidate the structural basis of the endonuclease V catalytic and recognition mechanism, we have performed alanine scanning mutagenesis at nine conserved positions of Tma endonuclease V. D43 and D110, along with E89, may coordinate metal ion(s) for the scissile phosphate bond hydrolysis and therefore are part of the active site. Y80 makes a substantial contribution to substrate and nicked product binding. While the lack of strong binding to substrate may account for loss of AP site and uracil cleavage activity, this same property also changes the kinetics of cleaving inosine-containing substrates such that the product release step is no longer rate-limiting. R88A and H116A affect binding steps as well, resulting in diminishing endonuclease activities toward non-inosine substrates. The lack of AP site and uracil cleavage suggests that K139A may affect steps other than substrate or product binding. Data obtained from this mutational study are consistent with a recently determined endo V crystal structure (A. M. Friedman, personal communication). Additional biochemical and structural studies will reveal more mechanistic details of endonuclease V.

ACKNOWLEDGMENT

We thank Drs. Don Bergstrom, Alan Friedman, Pat Paty, Wah Kow, Jie Tong, and Brian Kirk for discussions. We also thank GlaxoSmithKline for support and Michele Godlevski, Kay Boyle, and Su-Jun Deng for help.

REFERENCES

1. Huang, J., Lu, J., Barany, F., and Cao, W. (2001) *Biochemistry 40*, 8738−8748.
2. Yao, M., Hatahet, Z., Melamede, R. J., and Kow, Y. W. (1994) *J. Biol. Chem. 269*, 16260−16268.
3. Guo, G., and Weiss, B. (1998) *J. Bacteriol. 180*, 46−51.
4. Yao, M., Hatahet, Z., Melamede, R. J., and Kow, Y. W. (1994) *Ann. N.Y. Acad. Sci. 726*, 315−316.
5. Yao, M., and Kow, Y. W. (1994) *J. Biol. Chem. 269*, 31390−31396.
6. Yao, M., and Kow, Y. W. (1997) *J. Biol. Chem. 272*, 30774−30779.
7. Yao, M., and Kow, Y. W. (1996) *J. Biol. Chem. 271*, 30672−30676.
8. Bazar, L., Collier, G., Vanek, P., Siles, B., Kow, Y., Doetsch, P., Cunningham, R., and Chirikjian, J. (1999) *Electrophoresis 20*, 1141−1148.
9. Huang, J., Kirk, B., Favis, R., Soussi, T., Paty, P., Cao, W., and Barany, F. (2002) *Oncogene 21*, 1909−1921.
10. Neidhardt, F. C., Bloch, P. L., and Smith, D. F. (1974) *J. Bacteriol. 119*, 736−747.
11. Ho, S. N., Hunt, H. D., Horton, R. M., Pullen, J. K., and Pease, L. R. (1989) *Gene 77*, 51−59.
12. Lagunavicius, A., and Siksnys, V. (1997) *Biochemistry 36*, 11086−11092.
13. Fersht, A. (1985) *Enzyme structure and mechanism*, W. H. Freeman and Co., New York.
14. Porello, S. L., Leyes, A. E., and David, S. S. (1998) *Biochemistry 37*, 14756−14764.
15. Lane, D., Prentki, P., and Chandler, M. (1992) *Microbiol. Rev. 56*, 509−528.
16. Ljungquist, S. (1977) *J. Biol. Chem. 252*, 2808−2814.
17. Cao, W., and Barany, F. (1998) *J. Biol. Chem. 273*, 33002−33010.
18. Kim, D. R., Dai, Y., Mundy, C. L., Yang, W., and Oettinger, M. A. (1999) *Genes Dev. 13*, 3070−3080.
19. Kovall, R. A., and Matthews, B. W. (1999) *Curr. Opin. Chem. Biol. 3*, 578−583.
20. Deibert, M., Grazulis, S., Janulaitis, A., Siksnys, V., and Huber, R. (1999) *EMBO J. 18*, 5805−5816.
21. Cao, W., and Lu, J. (2001) *Biochim. Biophys. Acta 1546*, 253−260.
22. Vipond, I. B., Baldwin, G. S., and Halford, S. E. (1995) *Biochemistry 34*, 697−704.
23. Mol, C. D., Izumi, T., Mitra, S., and Tainer, J. A. (2000) *Nature 403*, 451−456.
24. Ausubel, F. M., Brent, R., Kingston, R. E., Moore, D. D., Seidman, J. G., Smith, J. A., and Struhl, K. (1997) *Current Protocols in Molecular Biology*, John Wiley & Sons, New York.

BI015960S